Journal of Global Change Data & Discovery. 2020, 4(4): 370-379
DOI:10.3974/geodp.2020.04.08
www.geodoi.ac.cn



# Net Primary Productivity Dataset of Mangrove Ecosystem in Guixian Island, China (2018)

Tao, J.[1] Tian, Y. C.[1,2*] Zhang, Q.[1] Zhou, G. Q.[2] Han, X.[1] Zhang, Y. L.[1]

1. School of Resources and Environment, Beibu Gulf University, Qinzhou 535011, China;
2. Guangxi Key Laboratory for Geospatial Informatics and Geomatics Engineering, Guilin University of Technology,Guilin 541004, China

**Abstract:** Based on the image data collected by drone seasonal aerial photography in 2018, as well as precipitation, temperature and solar radiation data from nearby weather stations, this research focusing on study into the Guixian Island and its adjacent areas have obtained the NPP dataset of mangrove ecosystem in Guixian Island of Beibu Gulf through introducing alternative visible-band difference vegetation index (VDVI) and adopting Carnegie–Ames–Stanford Approach (CASA) model to estimate the net primary productivity of vegetation. The data analysis results show that the spatial differences of vegetation NPP in different seasons are obvious. The seasonal increase percentages of NPP in the three stages of spring to summer, summer to autumn, and autumn to winter are 203.67%, –39.06% and –75.16%, respectively. In the NPP changes of the Guixian Island mangrove ecosystem, temperature has a stronger influence on NPP than precipitation. The dataset includes: (1) Landscape map of mangrove ecosystem study area in Guixian Island, Beibu Gulf in 2018 (.jpg). (2) Vegetation landscape types, VDVI vegetation index, seasonal scale and annual vegetation net primary productivity point data of mangrove ecosystem study area in Guixian Island, Beibu Gulf in 2018 (.shp). The dataset is archived in .jpg and .shp format with a data size of 15.5 MB (compression to 1 file, 3.11 MB).

**Keywords: drone; mangrove ecosystem; NPP; vegetation index; Beibu Gulf**

**Dataset Availability Statement:**

The dataset supporting this paper was published and is accessible through the *Digital Journal of Global Change Data Repository* at: https://doi.org/10.3974/geodb.2020.06.21.V1.

## 1 Introduction

Mangroves, which are one of the main types of "blue carbon" in coastal wetlands, grow on the intertidal tidal flats in tropical and subtropical regions. They have protection from wind

**Received:** 11-09-2020; **Accepted:** 02-12-2020; **Published:** 24-12-2020

**Foundations:** Guangxi Natural Science Foundation (2018JJA150135); Guangxi Innovation-driven Development Special Project (AA18118038); Guangxi Base and Talent Project (2019AC20088); Beibu Gulf University (2019KYQD28)

***Corresponding Author:** Tian, Y. C., School of Resources and Environment, Beibu Gulf University, tianyichao1314@yeah.net

**Data Citation:** [1] Tao, J., Tian, Y. C., Zhang, Q., *et al*. Net Primary productivity dataset of mangrove ecosystem in Guixian Island, China (2018) [J]. *Journal of Global Change Data & Discovery*, 2020, 4(4): 370–379. https://doi.org/10.3974/geodp.2020.04.08.

[2] Tao, J., Tian, Y. C., Zhang, Q., *et al*. Seasonal NPP dataset of the mangrove ecosystem in Guixian Island of China (2018) [J/DB/OL]. *Digital Journal of Global Change Data Repository*, 2021. https://doi.org/10.3974/geodb.2020.06.21.V1.

and waves, promote siltation and build land, purify the environment, provide transfer stations and food for migratory birds, and maintain ecological functions (such as biodiversity)[1–2]. Mangroves have very high carbon storage per unit area and are one of the ecosystems with the highest carbon content in tropical regions[2–3]. Therefore, the estimation of carbon storage in mangrove wetlands is important to assess the role of mangrove ecosystems in the global carbon cycle[4–6]. The mangrove communities in the Beibu Gulf of Guangxi are an important part of the mangrove wetland ecosystem in China. The mangroves of the Longmen Islands in Qinzhou are one of the most densely grown areas of mangroves in Qinzhou. Residential areas and many large-scale industrial areas surround it. The islands have long-term human activities. Thus, the study of the carbon storage and spatial distribution characteristics of the mangrove ecosystem of the Longmen Islands group under the interference of global climate change and human activities has important representativeness and typicality.

Net primary productivity (NPP) is the remaining part of the total organic matter produced by photosynthesis of green plants per unit time and area after deducting autotrophic respiration consumption[7]. Estimating changes in carbon storage depends on reliable estimates of NPP[8]. The models for estimating NPP mainly include statistical, parameter, and process models[9]. The Carnegie–Ames–Stanford approach (CASA) model of light energy utilization is a process-based remote sensing model that is used to estimate the NPP of ecosystems at global and regional scales. It is widely used in NPP estimation at global/region scale[7,9–15]. The present study adopts the CASA model improved by Zhu[7] on the basis of the UAV aerial image data in the four seasons of 2018 and the shared data of precipitation, temperature, and solar radiation from meteorological stations near the study area. The visible-band difference vegetation index (VDVI) is added to the estimated model parameters to estimate the NPP and its spatial distribution of vegetation in the mangrove ecosystem of Guixian Island in Beibu Gulf in different seasons.

## 2 Metadata of the Dataset

The metadata of the dataset[16] is summarized in Table 1. It includes the dataset full name, short name, authors, year of the dataset, temporal resolution, spatial resolution, data format, data size, data files, data publisher, and data sharing policy, etc.

## 3 Methods

As mentioned above, Zhu's improved CASA model[7] is used in this study. The parameters of the model are calculated on the basis of the RGB image data of the study area collected by drone aerial photography in the four seasons of spring, summer, autumn, and winter in 2018 and the shared meteorological data of precipitation, temperature, and solar radiation from meteorological stations near the study area provided by China Meteorological Sharing Service Network. With the help of CASA model[18], the NPP of mangrove ecosystem in Guixian Island is estimated, and the correlation analysis is conducted on the seasonal and monthly scales.

**Table 1** Metadata summary of the "Seasonal NPP dataset of the mangrove ecosystem in Guixian Island of China (2018)"

| Items | Description |
|---|---|
| Data full name | Seasonal NPP Dataset of the Mangrove Ecosystem in Guixian Island of China |
| Data short name | NPP_BeibuGulf Mangrove_2018 |
| Authors | Tao, J. AAT-4683-2020, School of Resources and Environment, Beibu Gulf University, taojin1216@yeah.net<br>Tian, Y. C., School of Resources and Environment, Beibu Gulf University, tianyichao1314@yeah.net<br>Zhang, Q. A-6449-2018, School of Resources and Environment, Beibu Gulf University, 676489898@qq.com<br>Zhou, G. Q., Guangxi Key Laboratory for Geospatial Informatics and Geomatics Enginee-ring, Guilin University of Technology, gzhou@glut.edu.cn<br>Han, X., School of Resources and Environment, Beibu Gulf University, 2383272519@qq.com<br>Zhang, Y. L., School of Resources and Environment, Beibu Gulf University, 641577425@qq.com |
| Geographical region | Guixian Island in Beibu Gulf (21°44′28″N–21°44′58″N, 108°35′24″E–108°35′44″E) |
| Year | 2018 |
| Temporal resolution | 1 season |
| Spatial resolution | 0.5 m |
| Data format | .jpg, .shp |
| Data size | 15.5 MB (Compressed to 3.11 MB) |
| Data files | (1) Landscape map of mangrove ecosystem study area in Guixian Island, Beibu Gulf in 2018 (.jpg). (2) Vegetation landscape types, VDVI vegetation index, seasonal scale and annual vegetation net primary productivity point data of mangrove ecosystem study area in Guixian Island, Beibu Gulf in 2018 (.shp) |
| Foundation(s) | Guangxi Natural Science Foundation (2018JJA150135); Guangxi Innovation-driven Development Special Project (AA18118038); Guangxi Base and Talent Project (2019AC20088); Beibu Gulf University High-level Talent Introduction Project (2019KYQD28) |
| Data computing environment | ArcGIS10.2, ENVI5.3 |
| Data publisher | Global Change Research Data Publishing & Repository, http://www.geodoi.ac.cn |
| Address | No. 11A, Datun Road, Chaoyang District, Beijing 100101, China |
| Data sharing policy | ***Data*** from the Global Change Research Data Publishing &Repository includes metadata, datasets (in the *Digital Journal of Global Change Data Repository*), and publications (in the *Journal of Global Change Data & Discovery*). ***Data*** sharing policy includes: (1) ***Data*** are openly available and can be free downloaded via the Internet; (2) End users are encouraged to use ***Data*** subject to citation; (3) Users, who are by definition also value-added service providers, are welcome to redistribute ***Data*** subject to written permission from the GCdataPR Editorial Office and the issuance of a ***Data*** redistribution license; and (4) If ***Data*** are used to compile new datasets, the 'ten per cent principal' should be followed such that ***Data*** records utilized should not surpass 10% of the new dataset contents, while sources should be clearly noted in suitable places in the new dataset[17] |
| Data and paper retrieval system | DOI, DCI, CSCD, WDS/ISC, GEOSS, China GEOSS, Crossref |

### 3.1 Study Area

The mangrove wetland of the Longmen Islands in Qinzhou is one of the four major wetlands in the Qinzhou Bay, and it is included in the list of important wetlands in China. This study selects Guixian Island in the Longmen Islands and its adjacent Beifengdun and the surrounding mangrove wetland community as the study area. Tourist facilities, such as a roundabout road, amusement wharf, and wind wheel platform, are available on the island with a total area of 27.08 $km^2$; they are accompanied by long-term human activities. The

image map and DEM of the study area are shown in Figure 1.

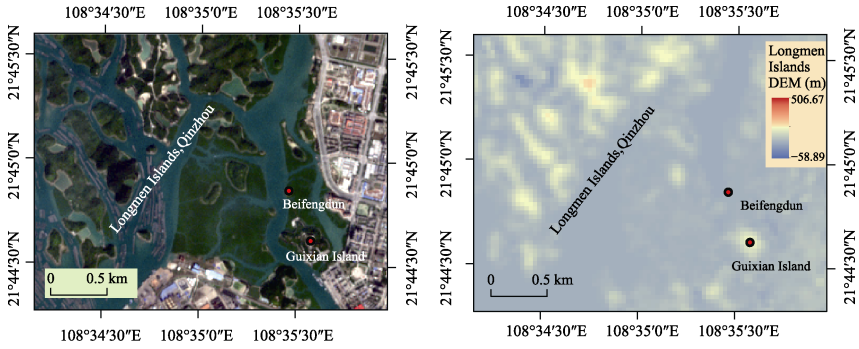


**Figure 1** Image and DEM Map of Guixian Island in Beibu Gulf

### 3.2 Algorithm Model

The CASA model is mainly determined by the two factors of plant absorbed photosynthetic active radiation (APAR) and actual light energy utilization (ε), and its estimation formula[7] is given as follows:

$$NPP(x,t) = APAR(x,t) \times \varepsilon(x,t) \quad (1)$$

where $NPP(x,t)$ is the NPP of the vegetation on the pixel $x$ in month $t$ ($t \cdot hm^{-2} \cdot a^{-1}$); $APAR(x,t)$ is the photosynthetically active radiation absorbed by the vegetation on the pixel $x$ in month $t$ ($MJ \cdot m^{-2}$); $\varepsilon(x,t)$ is the actual light energy utilization rate of the ground vegetation on the pixel $x$ in month $t$ ($gC \cdot MJ^{-1}$).

The APAR of plants depends on the total solar radiation and the absorption ratio of photosynthetically active radiation by vegetation; the absorption ratio of the photosynthetically active radiation is highly correlated with the VDVI[18]. The actual light energy utilization rate represents the efficiency of vegetation converting the absorbed photosynthetically active radiation into organic carbon[9], which is mainly affected by the low- and high-temperature stress coefficient, water stress coefficient, and maximum light energy utilization rate.

### 3.3 Data Processing

The acquisition and processing of relevant data in the study area and model parameter estimation are the core parts in applying the CASA model to estimate vegetation NPP. The data obtained in the early stage include (1) UAV images and control point data in the study area; (2) DEM data in the study area; and (3) meteorological data, such as precipitation, temperature, and solar radiation, in the study area. Data processing mainly includes UAV image data processing, meteorological data processing, and model parameter estimation.

#### 3.3.1 UAV Remote Sensing Image Collection and Processing

This study uses the regional scale to investigate the NPP of the Guixian Island mangrove wetland. The estimation model based on remote sensing is currently the most effective way to estimate the regional scale, but remote sensing data with different spatial resolutions will exert spatial scale effects. According to the relative altitude formula in the "Low-Altitude Digital Aerial Photography Specification", $H=f \times GSD/a$, where $H$ is the relative altitude, $f$ is the focal length of the camera lens, ground sample distance (GSD) is the ground sampling interval, and $a$ is the size of the pixel. Therefore, the same model of drone (DJI Phantom 4Pro) and the same planned route are used to collect data in the case of a fixed survey area.

Thus, the collected data have nearly the same GSD to effectively avoid the scale effect brought by the estimation of NPP based on remote sensing technology estimation model.

(1) Route planning and aerial photography data collection

UAV visible light remote sensing data collection usually selects a time zone around noon when the air visibility and light conditions are good and no wind or breeze exists. Therefore, the route should be planned in advance according to the location and terrain of the survey area. As shown in Figure 2, an aerial survey area of 578,191.97 $m^2$ is delineated using the DJI Terra ground station, the mission height is set to 100 m, the flying speed is 8 $m \cdot s^{-1}$, the GSD is fixed at 2.74 cm per pixel, the side overlap rate is 64%, the heading overlap rate is 80%, the main course angle is 180°, and the camera selects farmland white balance and automatic exposure mode. Every aerial photography mission throughout the year is conducted using the current route with fixed parameters.

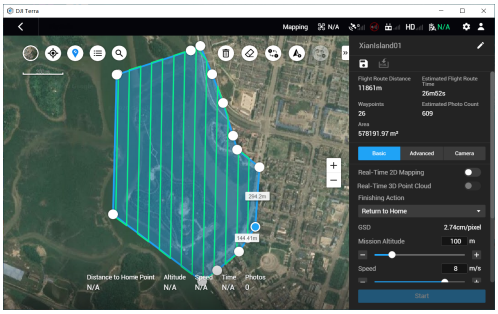


**Figure 2** Map of mangrove study area in Guixian Island

(2) Image control point selection

Image control points are ground points that can be clearly distinguished from the images and geo-coordinated then. The DJI Phantom 4Pro used in this experiment does not have an RTK module. Thus, image control points should be set up near the flight belt to ensure the accuracy of its relative position. Guixian Island is a tourist attraction, and the surrounding mangroves grow densely in the intertidal zone. Thus, the method of selecting the post-image control point uses a fixed parking lot angle that is close to a right-angle shape and a level that is close to a horizontal. The obvious landmarks at the intersection of the fixed road are also used as the image control point. The GeoMax Zenith15 Pro RTK is used to measure the precise geographic coordinates of the selected image control points, as shown in Figure 3. Seven image control points are collected in this experiment.

(3) Image control point import and thorn point processing

In using Terra 2D reconstruction, photos are added to the project (Figure 4). Then, image control points are imported, of which five are used as control points and two are used as check points. After the import is completed, the image control points will be displayed on the empty three views and in the image control point list, as shown in Figure 5. Any image control point can be selected, and an image that contains control point in the photo library can be clicked. The thorn point view will appear in the left area of the empty three views, and the blue crosshair indicates the predicted position of the selected image control point. The mouse position of the yellow front sight can be moved, and a puncture point can be created by clicking. The green front sight is the manual marking position. In spike point file export, the export control point button on the image control point view can be clicked to export the image control point and splinter point as a json file for each voyage mission containing the same splinter point image in the Guixian Island study area.

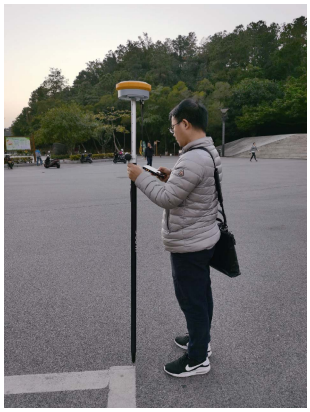

**Figure 3** Photo of *in situ* survey in Guixian Island

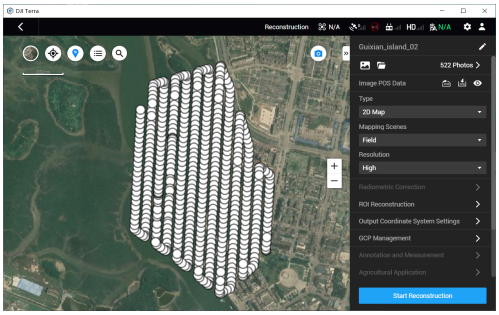


**Figure 4** Aerial photo loading map of Guixian Island mangrove research area

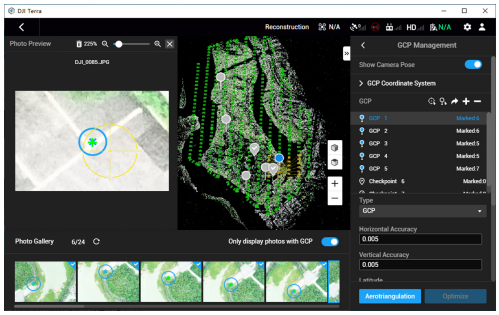


**Figure 5** Image control point import and thorn point processing view

(4) Analytical aerial triangulation and optimization and 2D reconstruction

After the thorn points of aerial triangulation are analyzed, the button can be clicked to perform aerial triangulation optimization solution. After completion, any image control point can be selected to view the re-projection error and 3D point error after aerial triangulation optimization. If the 3D point error is large, then the thorn point can be adjusted and the aerial triangulation optimization can be performed again until the error result meets the demand. The seven control point re-projection errors and 3D point errors are shown in the following table.

(5) Orthophoto processing

The results of the visible orthophoto of the Guixian Island study area are obtained for ROI cropping, and the vector boundary is saved for each subsequent orthophoto cropping and DEM cropping of the study area. The CART method in ENVI5.3 software is used to classify and interpret the cropped data. The results of the landscape pattern map of the study area are obtained by combining the unsupervised classification ISO data, VDVI index, texture features of mangrove communities, and original orthophotos with band synthesis and layer stacking.

### 3.3.2 Meteorological Data Processing

Point data (such as precipitation, temperature, and solar radiation) shared by meteorological sites are input into ArcGIS software. Software interpolation tools are used to perform Kriging interpolation processing to obtain the raster data of meteorological elements of monthly precipitation, monthly temperature, and monthly solar radiation in the study area with spatial resolution. The projection is consistent with the NPP data.

**Table 2** Image control point re-projection errors and 3D point errors

| Image control point name | Re-projection error (px) | 3D point error (m) |
|---|---|---|
| Control point1 | 0.156 | 0.003 |
| Control point2 | 0.205 | 0.011 |
| Control point3 | 0.421 | 0.016 |
| Control point4 | 0.304 | 0.029 |
| Control point5 | 0.412 | 0.009 |
| Control point6 | 0.455 | 0.026 |
| Control point7 | 0.297 | 0.022 |

### 3.3.3 Model Parameter Estimation

The CASA model parameter estimation is mainly calculated by inputting the pre-processed UAV image landscape classification data, VDVI vegetation index raster data, and meteorological raster data (such as precipitation, temperature, and solar radiation) and the study area DEM data into the model formula. The technical route is shown in Figure 6.

# 4 Data Results and Validation

## 4.1 Dataset Composition

The dataset include (1) the landscape map of Guixian Island mangrove ecosystem study area in Beibu Gulf in 2018 (.jpg); and (2) the vegetation landscape type, VDVI vegetation index, seasonal scale, and annual NPP data of vegetation in the Guixian Island mangrove ecosystem study area in Beibu Gulf in 2018 (.shp). In the corresponding attribute table, the field FID is an automatically generated field in generating the attribute table to ensure the continuity of the element number. The field "Shape" indicates that the vector data type is point type "Point". The field VDVI indicates the visible light waveband difference vegetation corresponding to the current point Index VDVI value. The fields NPP_Spring, NPP_Summer, NPP_Autumn, NPP_Winter, and NPP_Year represent the current point of spring, summer, autumn, and winter season scale and annual vegetation NPP. The field Landscapes represents the vegetation landscape type of the current point, and its value is an integer in the range of [1,10], which correspond to *Aegiceras corniculatum*, *Avicennia marina*, *Kandelia obvolata*, mudflat, water body, construction land, road, grassland, shrub, and woodland in the vegetation landscape types. The dataset consists of nine data files, which are placed in the first level folder of NPP_BeibuGulfMangrove_2018 through two second-level folders.

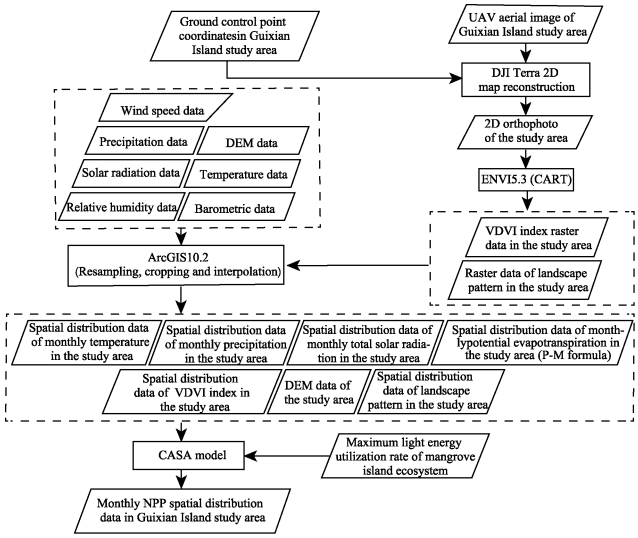


**Figure 6** Flow chart of dataset development

## 4.2 Data Results

With the increases in solar radiation, temperature, and precipitation in the Beibu Gulf in summer, Table 3 shows that the total NPP season in the Guixian Island study area reaches the highest value of 23,034,806.48 $gC \cdot m^{-2}$ in summer. This value is an increase of 203.67% compared with the total NPP season in spring. With the weakening of solar radiation, temperature reduction, and precipitation reduction from summer to autumn and from autumn to winter, the total amount of the autumn NPP decreases by 39.06% and the winter NPP decreases by 75.16% from the previous season. The total amount of NPP in the winter reaches the lowest value of 3,487,854.52 $gC \cdot m^{-2}$.

**Table 3** Statistics of NPP seasonal characteristic values of mangrove ecosystem in Guixian Island in 2018

| No. | Season | Seasonal minimum NPP ($gC \cdot m^{-2} \cdot a^{-1}$) | Seasonal maximum NPP ($gC \cdot m^{-2} \cdot a^{-1}$) | Seasonal average NPP ($gC \cdot m^{-2} \cdot a^{-1}$) | Seasonal total NPP ($gC \cdot m^{-2} \cdot a^{-1}$) | Percentage increase from last quarter (%) |
|---|---|---|---|---|---|---|
| 1 | spring | 0 | 241.05 | 62.98 | 7,585,396.78 | – |
| 2 | summer | 0 | 647.97 | 191.26 | 23,034,806.48 | 203.67 |
| 3 | autumn | 0 | 452.26 | 116.56 | 14,038,513.68 | –39.06 |
| 4 | winter | 0 | 110.68 | 28.96 | 3,487,854.52 | –75.16 |

The seasonal increase of NPP in the three stages of spring–summer, summer–autumn, autumn–winter in 2018 is visualized to study the seasonal changes of NPP more intuitively. As shown in Figure 7, the NPP increment in the study area from spring to summer is positive, and the range is [0, 527.62]. From summer to autumn, the NPP increment in the study area is

negative, and the range is [−443.49, 0]. From autumn to winter, the NPP increment in the study area is negative, and some vegetation types are accompanied by weak positive growth (the mangrove community is queried by the table), and the range is [−312.04, 19.18]. As shown in Figure 7, the area with the most dramatic seasonal NPP changes is the mangrove community between Guixian Island and Beifengdun relative to the vegetation community above the island. This community is divided into three sub-communities by small tidal trenches. On the whole, the NPP increments of the mangrove communities between the island piers are stronger in the west and weaker in the east. Its community habitat shows that there is a large tidal trench in the west side near the sea, and there is a large tidal trench in the east side near the shore. It is indicated that more suitable salinity conditions for mangrove growth is in the west side.

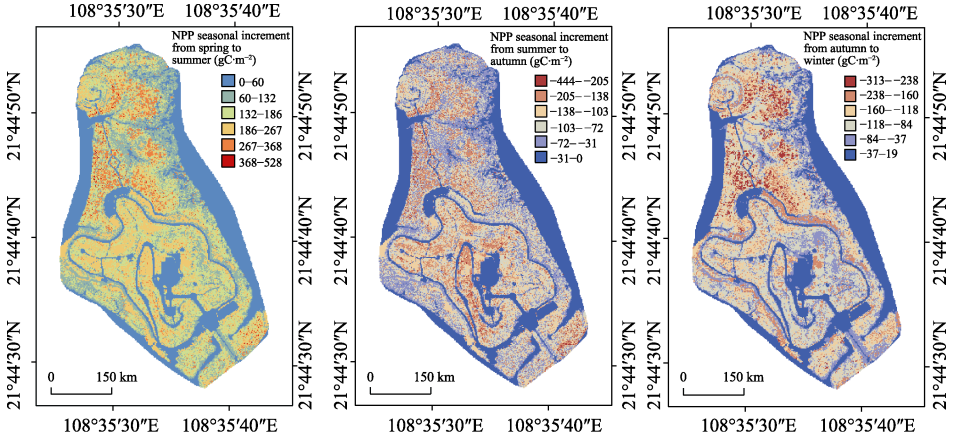


**Figure 7** NPP seasonal increment map of mangrove ecosystem in Guixian Island in the three stages of spring-summer, summer-autumn, autumn-winter in 2018

The estimation of vegetation NPP is affected by vegetation type, solar radiation, temperature, and precipitation. To determine the correlation between NPP and temperature and precipitation in the mangrove ecosystem of Guixian Island, the data of NPP, precipitation, and temperature in this area in December 2018 are statistically analyzed. As shown in Table 4, January is an extremely cold month and also the month with the lowest precipitation. It reaches the annual lowest temperature of 15.47 °C and has the lowest precipitation of 21.9 mm and the lowest NPP value of 6.83 gC·m$^{-2}$. June is an extremely hot month and has an annual maximum temperature of 29.34 °C. July is the month with the highest precipitation that reaches 748.3 mm.

**Table 4** Monthly NPP, precipitation and temperature data of Guixian Island mangrove research area in 2018

| Month | NPP (gC·m$^{-2}$) | Precipitation (mm) | Temperature (°C ) |
|---|---|---|---|
| 1 | 6.83 | 21.9 | 15.47 |
| 2 | 8.26 | 27.92 | 17.82 |
| 3 | 10.54 | 32.51 | 20.08 |
| 4 | 18.69 | 53.06 | 23.74 |
| 5 | 33.8 | 148.24 | 28.29 |
| 6 | 41.32 | 226.88 | 29.34 |
| 7 | 64.4 | 748.3 | 28.15 |
| 8 | 85.69 | 211.43 | 28.67 |
| 9 | 45.04 | 236.7 | 27.45 |
| 10 | 39.75 | 70.36 | 25.05 |
| 11 | 31.88 | 272.98 | 22.59 |
| 12 | 13.89 | 130.98 | 15.92 |

Correlation and regression analyses of the data in Table 4 indicate that the correlation coefficient between NPP and temperature is 0.81, the correlation coefficient between NPP and precipitation is 0.64, the *P* value of NPP and temperature is 0.001,5, and the *P* value of NPP and precipitation is 0.026,5. As observed, NPP and temperature have a very significant positive correlation. A generally significant positive correlation exists

between NPP and precipitation. Therefore, in the NPP changes of the Guixian Island mangrove ecosystem, the influence of temperature on NPP is stronger than that of precipitation. From the regional scale of the mangrove island ecosystem in Qinzhou Bay, this conclusion further verifies the research viewpoints in literature [19] and [20] that temperature is the main controlling factor of vegetation NPP in the coastal area of Beibu Gulf.

The monthly NPP values in January (very cold month and month with the lowest precipitation), June (extremely hot month), and July (the month with the highest precipitation) are visualized into a map in Figure 8. The figure shows that the highest NPP value of the entire Guixian Island mangrove ecosystem appears in the mangrove area between the islands regardless of the month with the lowest or highest temperature and the month with the lowest or precipitation.

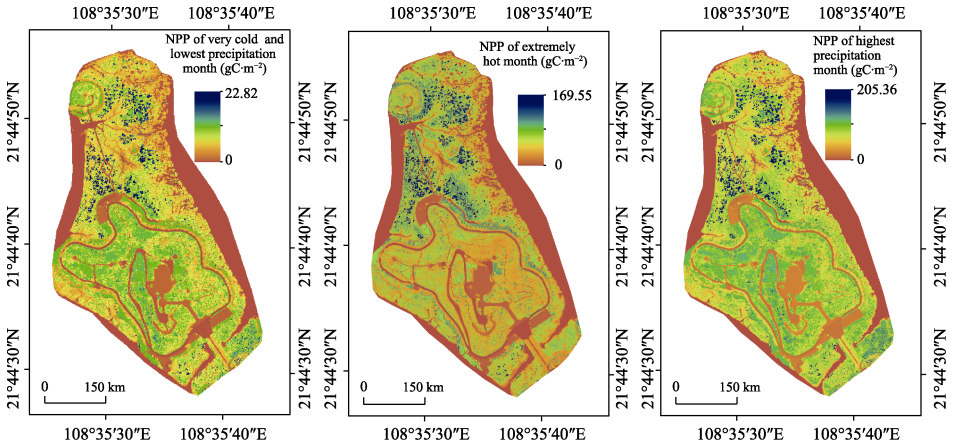


**Figure 8** Comparison of NPP between extreme temperature month and extreme precipitation month in Guixian Island in 2018

## 5 Discussion and Conclusion

This dataset is based on UAV remote sensing RGB data and related meteorological data (such as solar radiation, temperature, and precipitation). The NPP of mangrove communities and their spatial distribution are estimated by introducing the substitution vegetation index VDVI parameter into the CASA model formula. Obvious spatial differences in vegetation NPP are observed in the study area during the four seasons. The seasonal increase percentages of NPP in the three stages of spring to summer, summer to autumn, and autumn to winter are 203.67%, −39.06%, and −75.16%, respectively. Statistics of the NPP, precipitation, and temperature data of the study area in the 12 months of 2018 show that NPP has a very significant positive correlation with temperature and has a generally significant positive correlation with precipitation. In conclusion, in the NPP changes of Guixian Island mangrove ecosystem, the influence of temperature on NPP is stronger than that of precipitation. Subsequent research will consider the use of drones equipped with multi-spectral cameras in the same area to obtain NDVI index information. The accuracy of VDVI alternative parameters will also be evaluated through comparative studies.

### *Author Contributions*

Tao, J. and Tian, Y. C. designed the study. Tao, J., Zhang, Q., and Zhang, Y. L. contributed to the data processing and analysis. Tian, Y. C., and Zhou, G. Q. designed algorithm. Han, X. finished the data validation. Tao, J. wrote the data paper.

## References


[1] Jiang, L. Z., Yang, D. Y., Mei, L. Y., *et al*. Remote sensing estimation of carbon storage of mangrove communities in Shenzhen city [J]. *Wetland Science*, 2015, 13(3): 338–343.

[2] Peng, C. J., Qian, J. W., Guo, X. D., *et al*. Vegetation carbon stocks and net primary productivity of the mangrove forests in Shenzhen, China [J]. *Chinese Journal of Applied Ecology*, 2016, 27(7): 2059–2065.

[3] Zhang, L., Guo, Z. H., Li, Z. Y. Carbon storage and carbon sink of mangrove wetland: research progress [J]. *Chinese Journal of Applied Ecology*, 2013, 24(4): 1153–1159.

[4] Alongi, D. M. Carbon cycling and storage in mangrove forests [J]. *Annual Review of Marine Science*, 2014, 6(1): 195-219.

[5] Doughty, C. L., Langley, J. A., Walker, W. S., *et al*. Mangrove range expansion rapidly increases coastal wetland carbon storage [J]. *Estuaries and Coasts*, 2016, 39(2): 385–396.

[6] Hua, L., Li, W. Y., Xu, B. Monitoring mangrove forest change in China from 1990 to 2015 using Landsat-derived spectral-temporal variability metrics [J]. *International Journal of Applied Earth Observation and Geoinformation*, 2018, 73(1): 88–98.

[7] Zhu, W. Q., Pan, Y. Z., Zhang, J. S. Estimation of net primary productivity of Chinese terrestrial vegetation based on remote sensing [J]. *Chinese Journal of Plant Ecology*, 2007, 31(3): 413–424.

[8] Bolinder, M. A., Janzen, H. H., Gregorich, E. G., *et al*. An approach for estimating net primary productivity and annual carbon inputs to soil for common agricultural crops in Canada [J]. *Agriculture, Ecosystems and Environment*, 2007, 118: 29–42.

[9] Piao, S. L., Fang, J. Y., Guo, Q. H. Terrestrial net primary production and iIts spatio-temporal patterns in China during 1982–1999 [J]. *Acta Scientiarum Naturalium Universitatis Pekinensis*, 2001(4): 563–569.

[10] Piao, S. L., Fang, J. Y., Guo, Q. H. Application of CASA model to the estimation of Chinese terrestrial net primary productivity [J]. *Chinese Journal of Plant Ecology*, 2001(5): 603–608, 644.

[11] Zhang, F., Zhou, G. S., Wang, Y. H. Dynamics simulation of net primary productivity by a satellite data driven CASA model in inner Mongolia typical steppe, China [J]. *Chinese Journal of Plant Ecology*, 2008(4): 786–797.

[12] Tian, Y., C., Huang, Y. L., Zhang, Q., *et al*. Spatiotemporal distribution of net primary productivity and its driving factors in the Nanliu River basin in the Beibu Gulf [J]. *Acta Ecologica Sinica*, 2019(21): 8156–8171.

[13] Schaefer, K., Collatz, G. J., Tans, P., *et al*. Combined simple Biosphere/Carnegie-Ames-Stanford approach terrestrial carbon cycle model [J]. *Journal of Geophysical Research*, 2008, 113: G03034.

[14] Cao, S., Sanchez-Azofeifa, G. A., Duran, S. M., *et al*. Estimation of aboveground net primary productivity in secondary tropical dry forests using the Carnegie–Ames–Stanford approach (CASA) model [J]. *Environmental Research Letters*, 2016, 11: 075004.

[15] Donmez, C., Berberoglu, S., Curran, P. J. Modelling the current and future spatial distribution of NPP in a Mediterranean watershed [J]. *International Journal of Applied Earth Observation and Geoinformation*, 2011, 13: 336–345.

[16] Tao, J., Tian, Y. C., Zhang, Q., *et al*. Net primary productivity dataset of mangrove ecosystem in Guixian Island, Beibu Gulf (2018) [J/DB/OL]. *Digital Journal of Global Change Data Repository*, 2020. https://doi.org/10.3974/geodb.2020.06.21.V1.

[17] GCdataPR Editorial Office. GCdataPR data sharing policy [OL]. https://doi.org/10.3974/dp.policy.2014.05 (Updated 2017).

[18] Tian, Y., C., Huang, Y. L., Tao, J., *et al*. Estimation of net primary productivity of typical mangrove and archipelago ecosystems in the Beibu Gulf based on unmanned aerial vehicle imagery [J]. *Tropical Geography*, 2019(4): 583–596.

[19] Tian, Y., C., Liang, M. Z., The NDVI characteristics of vegetation and its ten-day response to temperature and precipitation in Beibu Gulf coastal region [J]. *Journal of Natural Resources*, 2016(3): 488–502.

[20] Tian, Y., C., Huang, Y. L., Zhang, Q., *et al*. Spatiotemporal distribution of net primary productivity and its driving factors in the Nanliu River basin in the Beibu Gulf [J]. *Acta Ecologica Sinica*, 2019, 21: 8156–8171.